

# Crystal structures and photoreactivity of *trans*- and *cis*-valerophenone diperoxides

Hiroki Takahashi · Yoshikatsu Ito

Received: 23 May 2011 / Accepted: 20 September 2011 / Published online: 9 October 2011  
© Springer Science+Business Media, LLC 2011

**Abstract** The crystal structures of valerophenone diperoxides *trans*-**1** and *cis*-**1** were elucidated by X-ray crystallographic analysis. The 1,2,4,5-tetraoxane rings of both compounds adopt chair conformations. Intermolecular CH...O hydrogen bond,  $\pi$ - $\pi$ , and CH/ $\pi$  interactions exist in *cis*-**1**, whereas only CH/ $\pi$  interactions exist in *trans*-**1**. In the asymmetric unit of the crystal, a half molecule exists for *trans*-**1**, while one molecule for *cis*-**1** which shows whole-molecule disorder. Solid-state photolysis (at 254 nm) or solution-state thermolysis (at 150 °C) of *trans*-**1** and *cis*-**1** produced valerophenone (**2**) and butyl benzoate (**3**). Rationalization of the solid-state photoreactivity of the diperoxides by their crystal structures was attempted.

**Keywords** 1,2,4,5-Tetraoxane · X-ray analysis · Intermolecular interaction · Photolysis · Thermolysis

## Introduction

Studies on the crystal structure–reactivity correlation are fundamentally important, because the reactivity and the product stereochemistry are predictable from the crystal structure [1–3]. Aiming at achieving desired solid-state

reactions, a variety of investigations to manipulate the crystal structures through supramolecule formation were conducted: for instance, organic salts by Scheffer [1–3], host–guest crystals by Toda [4, 5], photodimerization in templates by MacGillivray [6–8], and designed topochemical polymerization by Lauher [9]. One of the present authors also contributed several papers for this purpose (vide infra).

Recently, some 1,2,4,5-tetroxane derivatives containing a diperoxide structure were found to exhibit remarkable antimalarial activities in vitro and in vivo [10–12]. This activity is probably associated with the reactivity of the peroxide group and the steric and electronic effects of the substituents surrounding the diperoxide group. For this reason, new synthetic methods, structure and reactivity of cyclic diperoxides have been investigated [13, 14].

Preparation of *trans*-valerophenone diperoxide (*trans*-**1**) and *cis*-valerophenone diperoxide (*cis*-**1**) (Scheme 1) and their thermal and photosensitized decomposition in solution were previously reported [15–18]. In continuation of these studies, it has been found that the thermal decomposition of *cis*-**1** is faster than that of *trans*-**1** in solution, whereas their relative rates are reversed under direct photolysis in the crystalline state. In order to interpret this contrary relative stability of *trans*-**1** and *cis*-**1**, we now elucidated their crystal structures. The results are reported below.

H. Takahashi (✉)

Department of Interdisciplinary Environment, Graduate School of Human and Environmental Studies, Kyoto University, Kyoto 606-8501, Japan  
e-mail: takahashi.hiroki.2x@kyoto-u.ac.jp

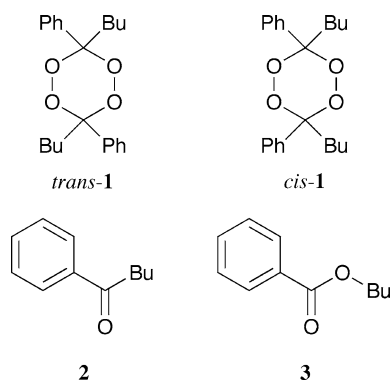
Y. Ito

Department of Synthetic Chemistry and Biological Chemistry, Graduate School of Engineering, Kyoto University, Katsura, Kyoto 615-8510, Japan  
e-mail: yito@sbchem.kyoto-u.ac.jp

## Experimental

### Synthesis

*Trans*- and *cis*-valerophenone diperoxides (*trans*-**1** and *cis*-**1**) were previously prepared [15–17]. These samples were purified by preparative TLC (silica gel, CCl<sub>4</sub>), followed by recrystallization from *n*-pentane.



**Scheme 1** Chemical structure of valerophenone diperoxides *trans*-1, *cis*-1, and the products **2** and **3**

### X-ray crystallography of *trans*-1 and *cis*-1

Suitable crystals of *trans*-1 and *cis*-1 to be used for X-ray analysis were obtained by recrystallization from *n*-pentane. The X-ray experiments were performed on a Rigaku Saturn724+ CCD area detector diffractometer mounted on a 1/4

$\chi$  goniometer (graphite-monochromated Mo K $\alpha$  radiation ( $\lambda = 0.71073$  Å);  $\omega$  scans) with a Rigaku low-temperature equipment. The data were collected at  $-173$  °C. The crystal structures were solved by direct methods (SIR97 [19]) and refined by full-matrix least-squares methods (SHELXL-97 [20]). All the non-hydrogen atoms were refined anisotropically, whereas the hydrogen atoms were refined using a riding model. With respect to crystal of *cis*-1, whole molecule was disordered, but constraints or restraints were not applied for any atom in the structure. All the calculations were performed using crystallographic software packages CrystalStructure [21] and Yadokari-XG 2009 [22]. Crystal data and details of the structure determination and refinement can be found in Table 1. The programs Mercury [23] and PLATON [24] were used for analysis of intermolecular interactions and for making graphics.

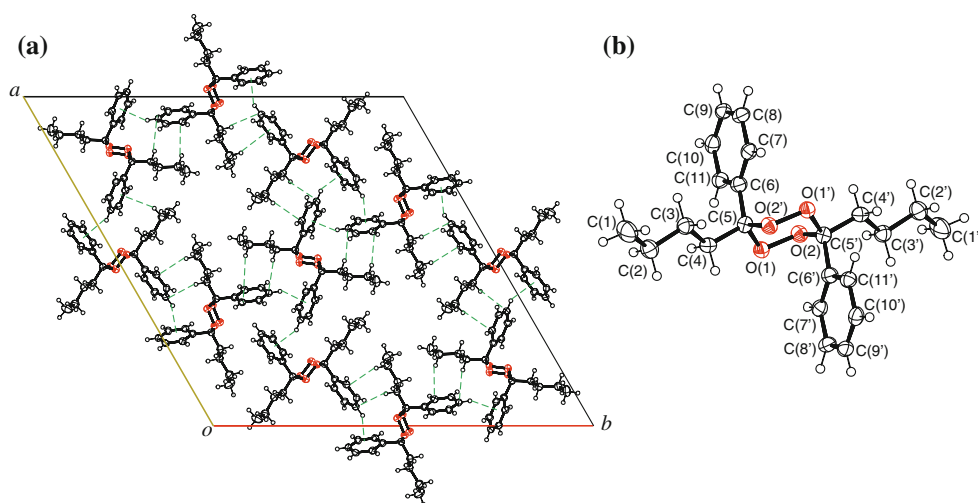
### Solid-state photolysis of *trans*-1 and *cis*-1

Irradiation was carried out with a 10-W low-pressure mercury lamp at 254 nm. HPLC analyses were performed

**Table 1** Crystal and experimental data

Compound	<i>Trans</i> -1	<i>Cis</i> -1
CCDC deposit no.	CCDC-787284	CCDC-787283
Color/shape	Colorless/needle	Colorless/prism
Empirical formula	C <sub>22</sub> H <sub>28</sub> O <sub>4</sub>	C <sub>22</sub> H <sub>28</sub> O <sub>4</sub>
Formula weight	356.44	356.44
Temperature, °C	$-173(1)$	$-173(1)$
Crystal system, space group	Trigonal, $R\bar{3}$	Monoclinic, $P2_1/n$
Unit cell dimensions		
<i>a</i> (Å)	30.426(3)	5.7850(19)
<i>b</i> (Å)	30.426(3)	21.258(7)
<i>c</i> (Å)	5.685(3)	15.973(5)
$\alpha$ (°)	90	90
$\beta$ (°)	90	94.802(6)
$\gamma$ (°)	120	90
<i>V</i> (Å <sup>3</sup> )	4557(6)	1957.5(11)
<i>Z</i>	9	4
Density (calculated), g/cm <sup>3</sup>	1.169	1.209
Absorption coefficient, mm <sup>-1</sup>	0.079	0.079
<i>F</i> (000)	1728	768
$\theta$ range for collection (°)	3.54–27.55	3.15–27.46
Reflections measured	12,597	31,767
Independent reflections	2326	4466
Index ranges $\pm h, \pm k, \pm l$	$-39 \leq h \leq 38, -39 \leq k \leq 39, -7 \leq l \leq 7$	$-7 \leq h \leq 7, -27 \leq k \leq 27, -20 \leq l \leq 20$
Data/restraints/parameters	2326/0/174	4466/0/473
Goodness of fit on $F^2$	1.110	1.120
Final <i>R</i> indicates [ $I > 2\sigma(I)$ ]	0.0389	0.0457
Final <i>R</i> <sub>w</sub> indicates [ $I > 2\sigma(I)$ ]	0.1132	0.0925

**Fig. 1** ORTEP drawings of *trans-1*: **a** crystal and **b** molecular structure with labeled atoms. Atoms with the suffix prime are generated by the symmetry operation  $(1 - x, -y, 1 - z)$ . Thermal displacement ellipsoids are drawn at 50% probability level. The H atoms are represented by spheres, and the intermolecular interactions ( $\text{CH}\cdots\pi$ ) are indicated by green broken lines



with a JASCO PU-980 pump and a SHIMADZU SPD-6AV detector by using a Cosmosil 5C<sub>18</sub>-AR column (4.6 mm i.d.  $\times$  150 mm) and were eluted (1 mL/min) with a mixture of MeOH–H<sub>2</sub>O (90:10 or 65:35 v/v).

Crystalline samples of *trans-1* and *cis-1* were crushed in an agate mortar and pestle with a similar strength, respectively. Then ca. 10 mg of each sample was placed in a special quartz vessel [25, 26] and was irradiated for 0.5 h under the stream of Ar gas at 0 °C. After the irradiation, the sample was dissolved in MeCN, followed by the addition of benzophenone as the standard to determine the amounts of **2** and **3**, and then the solution was analyzed with HPLC. Next, dibenzyl was added to the solution as the standard to determine the amount of *trans-1* or *cis-1*, and the solution was analyzed with HPLC.

In the case of the time-course experiments, ca. 10 mg of each sample was similarly irradiated. A tiny part of the sample was taken out after an appropriate irradiation time, and it was dissolved in MeCN. Then, the solution was directly analyzed with HPLC. The material balance of **1**, **2**, and **3** was assumed to be quantitative (total 100%). The decomposition of the diperoxides **1** stopped at low conversions and the HPLC retention times of **1** differed very much from those of **2** and **3** (retention times with 90/10 MeOH–H<sub>2</sub>O: *trans-1* 9.4, *cis-1* 8.2, **2** 2.6, **3** 3.0 min; retention times with 65/35 MeOH–H<sub>2</sub>O: *trans-1* > 60, *cis-1* > 60, **2** 10.8, **3** 18.9 min). Furthermore, irradiation of all parts of the solid sample equally was difficult with our set-up [25, 26], although the powder was mixed with a spatula from time to time. Therefore, determinations of the diperoxide recovery were subjected to large experimental errors as seen from Fig. 4.

#### Thermolysis of *trans-1* and *cis-1*

A solution of *trans*- or *cis*-**1** (0.05 M) in 1 mL of diphenyl ether was heated in an oil bath at 150 °C for 5 h. Then, the reaction mixture was analyzed with HPLC, as described above.

#### Results and discussion

*Trans-1* crystallizes in the trigonal space group  $R\bar{3}$ . One-half molecule exists in the asymmetric unit of *trans-1*. The 1,2,4,5-tetraoxane ring adopts a chair conformation (puckering parameter:  $Q = 0.634(1)$  Å,  $\theta = 179.17(1)^\circ$  and  $\phi = 0.00^\circ$ ) [27], and the Ph and Bu groups are axial and equatorial, respectively (Fig. 1b). CH/ $\pi$  interactions are observed between the Bu and the center of gravity of Ph groups (Cg) [C2–H5 $\cdots$ Cg<sup>i</sup> 3.19(2) Å and C4–H9 $\cdots$ Cg<sup>i</sup> 3.45(2) Å, (symmetry code: (i)  $1/3 + y, 2/3 - x + y, 2/3 - z$ ) and C9–H12 $\cdots$ Cg<sup>ii</sup> 2.82(2) Å, (symmetry code: (ii)  $4/3 - x + y, 2/3 - x, z - 1/3$ )] (Fig. 1a).

*Cis-1* crystallizes in the monoclinic space group  $P2_1/n$ . One molecule exists in the asymmetric unit of the crystal. The molecule shows whole-molecule disorder and has two conformational isomers (A and B) with occupancy factors of 0.55(2) and 0.45(2), respectively, as shown in Fig. 2b–e. The conformers A and B are virtually the same (Bu and Ph are axial and equatorial, respectively, in one half of the molecule, whereas they are equatorial and axial, respectively, in the other half), except that they have slightly different bond lengths and angles (Fig. 2e) so that the puckering parameters are  $Q = 0.646(2)$  Å,  $\theta = 1.3(2)^\circ$ , and  $\phi = 83(6)^\circ$  for conformer A;  $Q = 0.649(2)$  Å,  $\theta = 0.0(3)^\circ$ , and  $\phi = 65(7)^\circ$  for conformer B. Selected bond lengths and angles for *cis-1* are listed in Table 3. The average lengths of O–O and C–O in reported cyclic diperoxide derivatives are 1.472 and 1.436 Å, respectively.<sup>1</sup>

<sup>1</sup> Referring to the Cambridge Crystallographic Database (CSD Ver. 5.32), 21 crystals containing 1,2,4,5-tetraoxane have been reported. Their refcodes are as follows: AROZEM, BMTTRX, CEDDO, DPTOCH, GAGTEO, GAGTIS, GAHXIW, IBEJAA, LEVSOV, LEVSUB, MUPTTEW, QINDAS, QINDEW, QINDIA, SCHOCH10, SCHOHX10, SIFGAQ, SPOCTC10, SPOCTC10, VIBHIX, and YIZFET. We calculated the average bond lengths by using these data.

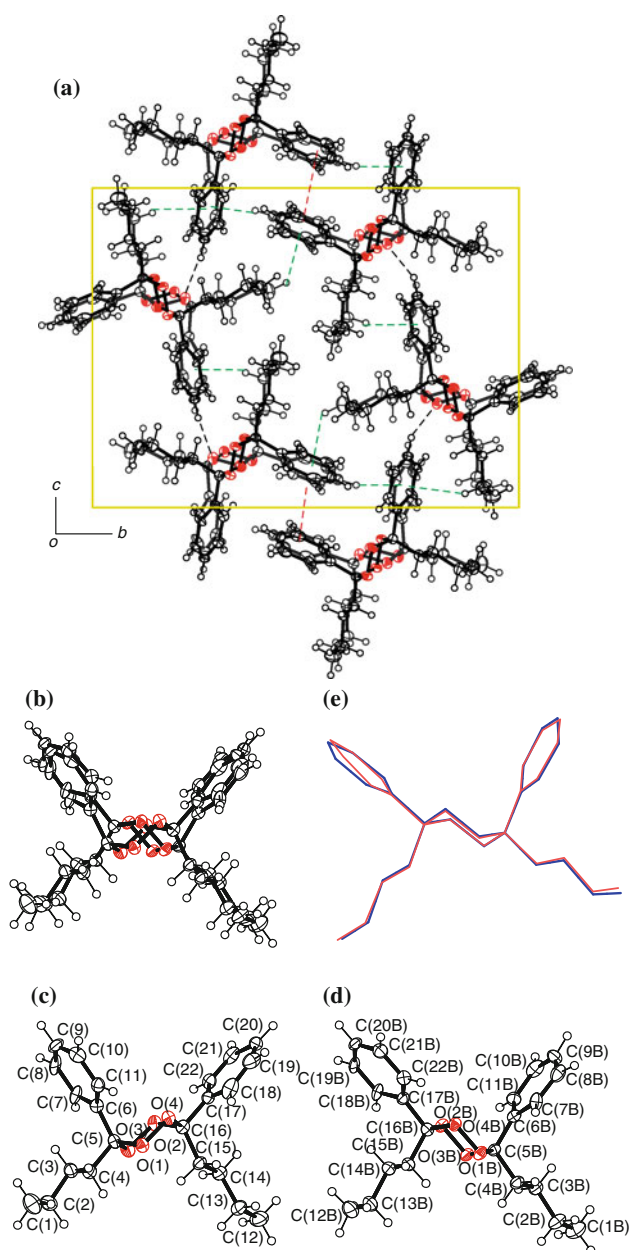


**Fig. 2** ORTEP drawings of *cis-1*: **a** crystal packing, **b** disordered form, **c** conformer A, **d** conformer B, and **e** overlay of the molecular structures of two disordered form by using AutoMolFit [28] (PLATON); the red and blue molecules correspond to conformers A and B, respectively. Thermal displacement ellipsoids are drawn at 50% probability level. The H atoms are represented by spheres, and the intermolecular interactions are indicated by black (CH $\cdots$ O), green (CH $\cdots$  $\pi$ ), and red ( $\pi\cdots\pi$ ) broken lines

The O–O and C–O bond lengths for both the conformers range from 1.470 to 1.486 Å and 1.421 to 1.444 Å, respectively, whereas the O–O and C–O bond lengths for *trans-1* are slightly shorter or equal to the average value, as given in Table 3.

Intermolecular CH $\cdots$ O hydrogen bond, CH/ $\pi$ , and  $\pi$ – $\pi$  interactions are observed for *cis-1* between the hydrogen

atom of phenyl group and tetraoxane oxygen atom [CH $\cdots$ O: 3.187 Å C20–H26 $\cdots$ O1<sup>iii</sup> (symmetry code: (iii)  $1/2 + x, 1/2 - y, -1/2 + z$ )], between the Bu and the center of gravity of Ph groups [CH/ $\pi$ : 2.986 Å C13B–H19B $\cdots$ Cg(Be)<sup>iv</sup> [For the detail of the two characters in parentheses, see note of Table 2.] (symmetry code: (iv)  $x - 1/2, 1/2 - y, 1/2 + z$ ), 2.780 Å C20B–H26B $\cdots$ Cg(Ae)<sup>v</sup> (symmetry code: (v)  $2 - x, -y, -1 - z$ ) and 2.83 Å C20B–H26B $\cdots$ Cg(Be)<sup>vi</sup> (symmetry code: (vi)  $2 - x, -y, -1 - z$ )], and between Ph groups [ $\pi$ – $\pi$ : Cg–Cg distance: 4.250(5) Å Cg(Aa)–Cg(Aa)<sup>vii</sup>, 3.977(6) Å Cg(Aa)–Cg(Be)<sup>vii</sup>, and 3.722(6) Å Cg(Be)–Cg(Be)<sup>vii</sup>; (symmetry code: (vii)  $2 - x, -y, -1 - z$ )], respectively. The detailed parameters and schematic representation of the  $\pi$ – $\pi$  interactions are shown in Table 2 and Fig. 3, respectively.

Equivalent isotropic displacement parameters ( $U_{eq}$ ) [29] for *cis-1* and *trans-1* were listed in Table 4. The averaged ratios of  $U_{eq}(cis)/U_{eq}(trans)$ , Ph, Bu and 1,2,4,5-tetraoxane group(s), which are calculated from the averaged  $U_{eq}$  values for each group of *cis-1* and *trans-1*, are 1.6, 1.2, and 1.3, respectively. The Ph groups for *cis-1* have large displacement parameters in the molecule. This result [ $U_{eq}(cis)/U_{eq}(trans)$  ratios > 1] indicates that the molecules in the *cis-1* crystal may have more librational motion than those in the *trans-1* crystal.

#### Reactivity of *trans-1* and *cis-1*

Irradiation of the diperoxide crystals of *trans-1* and *cis-1* with 254 nm light at 0 °C for a short time (0.5 h) led to their decomposition to a small extent and valerophenone (**2**) along with butyl benzoate (**3**) were produced as almost exclusive products with a molar ratio  $2/3 \gg 1$  (Eqs. 1 and 3 in Scheme 2). In a separate experiment, the time course of photolysis was examined for both diperoxides (Figs. 4, 5). It appears that at first *trans-1* decomposed more rapidly than *cis-1*, but the decompositions stopped after prolonged irradiation in both cases (maximum conversion  $\sim 6\%$ , Fig. 4). This may be attributed to the inner filter effect by the products (**2** and **3**), which were formed on the crystal surface and absorb efficiently the incident light (254 nm) (molar absorptivity  $\epsilon$  in ethanol at 254 nm: *trans-1* 520, *cis-1* 340, **2** 5200, **3** 1180 M<sup>-1</sup>cm<sup>-1</sup>). Figure 5 displays that the  $2/3$  ratio gradually decreased with the irradiation time. This decrease must have been caused by further photolysis of the product **2**, i.e., the product **2** was consumed by the concurrent Norrish type II photoreaction [30]. Because of various experimental difficulties (see “Experimental” section), the time-course experiments for the diperoxide recovery were subjected to large experimental errors, as seen from Fig. 4. Experiments presented in Eqs. 1 and 3 (Scheme 2) were carried out to confirm the

**Table 2** Geometrical parameters of  $\pi$ – $\pi$  interactions for *cis*-**1**

Cg(I)–Cg(J) <sup>a</sup>	Distance (Å)	$\alpha$ (°) <sup>b</sup>	$\beta$ (°) <sup>c</sup>	$\gamma$ (°) <sup>d</sup>	CgI_PP (Å) <sup>e</sup>	CgJ_PP (Å) <sup>f</sup>	Slippage (Å) <sup>g</sup>
Cg(Aa)–>Cg(Aa) <sup>vii</sup>	4.250(5)	0.0	35.06	35.06	3.479(4)	3.479(4)	2.441
Cg(Be)–>Cg(Be) <sup>vii</sup>	3.722(6)	0.0	25.38	25.38	3.362(4)	3.362(4)	1.595
Cg(Aa)–>Cg(Be) <sup>vii</sup>	3.977(6)	5.80	31.91	28.53	3.494(4)	3.376(4)	–

<sup>a</sup> Geometrical center of phenyl rings. The two characters in parentheses indicate the conformer (A or B) and the position of the phenyl ring (e: equatorial or a: axial), respectively. <sup>b</sup> Dihedral angle between phenyl planes I and J. <sup>c</sup> Angle between Cg(I) → Cg(J) vector and normal to plane I. Angle between the Cg(I) → Cg(J) vector and the vector normal to plane I. <sup>d</sup> Angle between Cg(I) → Cg(J) vector and normal to plane J. <sup>e</sup> Perpendicular distance of Cg(I) on ring J. <sup>f</sup> Perpendicular distance of Cg(J) on ring I. This distance corresponding to the interplanar distance. <sup>g</sup> Distance between Cg(I) and perpendicular projection of Cg(J) on ring I. Symmetry code (vii) (2 – x, –y, –1 – z)

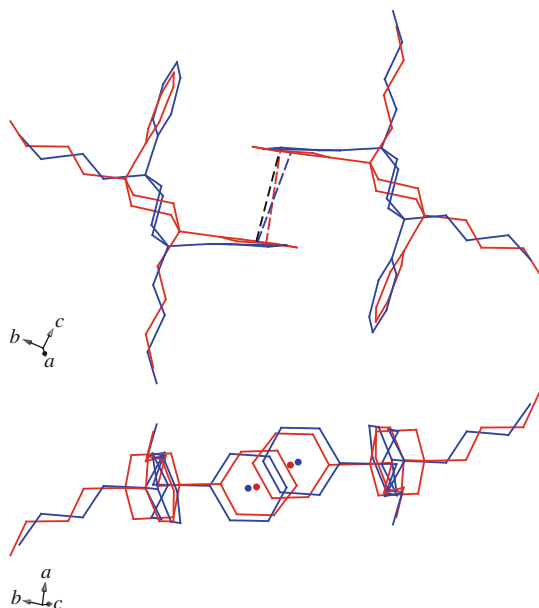


**Fig. 3** The schematic representation of  $\pi$ – $\pi$  interactions between the neighboring phenyl planes for *cis*-**1**: symmetry operation (2 – x, –y, –1 – z). The red and blue dots are the center of gravity for conformer A and B, respectively. The Cg–Cg distances are shown by red [Cg(Aa)–Cg(Aa), 4.250 Å], blue [Cg(Be)–Cg(Be), 3.722 Å], and black [Cg(Aa)–Cg(Be), 3.977 Å] broken lines, respectively. The interplanar distance 3.479 Å (conformer A, red) and 3.362 Å (conformer B, blue). Projections in two directions are shown. There is no such  $\pi$ – $\pi$  interaction for *trans*-**1**

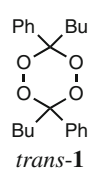
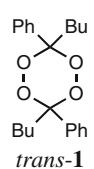
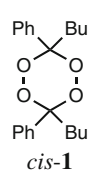
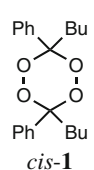
difference of initial photoreactivity between *trans*-**1** and *cis*-**1**. Now, from inspection of Eqs. 1 and 3 (Scheme 2) and Figs. 4, 5, it seems apparent that (a) the irradiation of *trans*-**1** gave nearly twice the **2/3** ratio than the irradiation of *cis*-**1** and (b) the initial stage of photochemical decomposition of *trans*-**1** was about three times faster than that of *cis*-**1**.

Thermolysis of *trans*-**1** and *cis*-**1** in diphenyl ether at 150 °C for 5 h was performed. Valerophenone (**2**) and butyl benzoate (**3**) were produced as major products (Eqs. 2 and 4 in Scheme 2). Formation of the previously reported byproducts such as phenyl valerate and 2-phenoxybiphenyl [15–18] was neglected. It can be noticed that,

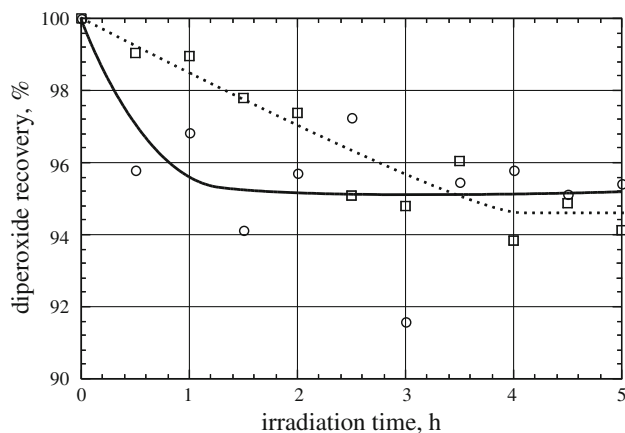
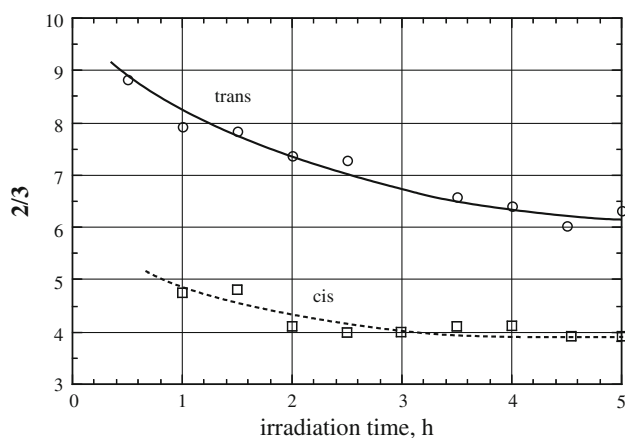
contrary to the above-mentioned solid-state photolysis, the decomposition of *cis*-**1** (conversion 82%) was faster than that of *trans*-**1** (conversion 38%). The **2/3** ratio from *trans*-**1** (2.8) was nearly twice larger than that from *cis*-**1** (1.5), but these ratios were considerably smaller when compared with the case of solid-state photolysis (4–10 from Eqs. 1, 3 and Fig. 5).

Thus, it was observed that (i) the **2/3** selectivity was always more than one (1.5–10), (ii) the **2/3** selectivity was considerably higher by the solid-state photolysis (4–10) than by the solution thermolysis (1.5–2.8), and (iii) the **2/3** selectivity from *trans*-**1** was nearly twice higher than that from *cis*-**1**. Photochemical or thermal decomposition of peroxidic compounds usually begins with cleavage of the weakest bond, i.e., a peroxide bond. Therefore, diperoxides *trans*-**1** and *cis*-**1** should decompose mainly from the O–O bond cleavage of path a in Scheme 3 [31–34]. It seems from the observation (i) that this mode of decomposition ends up with formation of **2** more than **3**. The observation (ii) is as expected, since the reaction is generally more selective in crystals than in a solution. Scheme 3 describes another possible decomposition pathway (path b), where the cleavage of two C–O bonds occurs first and the ensuing carbonyl oxide intermediate, as recently described in a review [35], leads mainly to the formation of ester **3**. It may be assumed that path b is occurring to some extent in the solution, since the **2/3** selectivity is low. The observed lower **2/3** selectivity from *cis*-**1** than from *trans*-**1** (the observation (iii)) may infer that *cis*-**1** has a somewhat stronger tendency to decompose through path b. It seems difficult to prove this inference on the basis of the present X-ray structures, because all the O–O and C–O bond lengths in the 1,2,4,5-tetraoxane ring of *cis*- and *trans*-**1** are normal and there are no clear features in the thermal parameters of the ring atoms (Tables 3, 4). However, a preliminary analysis of the X-ray data of *cis*-**1** at 0 °C, which will be published elsewhere, suggests that its 1,2,4,5-tetraoxane ring atoms are undergoing large librational motions at 0 °C. Large thermal vibrations at the ring carbon atoms of *cis*-**1** may be taken to induce the C–O

**Scheme 2** Reactivity of *trans*-**1** and *cis*-**1**

	conversion (%)	products (%)		2/3 (molar ratio)	
		Ph-OO-Bu (2)	Ph-CO-OBu (3)		
 <i>trans</i> - <b>1</b>	4.5	91	9	10	(1)
 <i>trans</i> - <b>1</b>	38	74	26 <sup>a</sup>	2.8	(2)
 <i>cis</i> - <b>1</b>	1.6	85	15	5.7	(3)
 <i>cis</i> - <b>1</b>	82	60	40 <sup>a</sup>	1.5	(4)

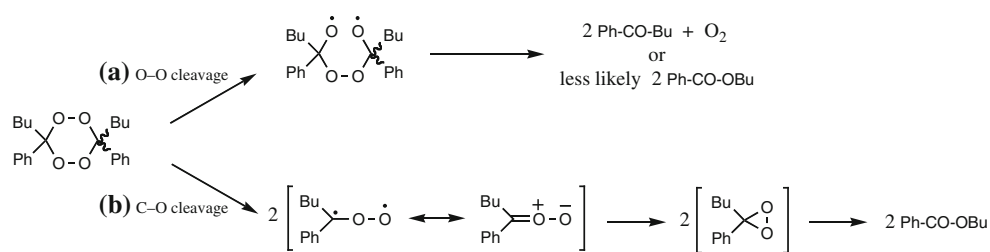
<sup>a</sup>The formation of by-products [15–18] was neglected.

**Fig. 4** Time-course of the decomposition for *trans*- or *cis*-valerophenone diperoxide (*trans*-**1** or *cis*-**1**) upon solid-state photolysis at 254 nm and 0 °C**Fig. 5** Change of the valerophenone/butyl benzoate (2/3) ratio with time upon solid-state photolysis of *trans*-**1** or *cis*-**1** at 254 nm and 0 °C

bond cleavage (the occurrence of path b). Further X-ray crystallographic and other work is desired along this line.

Previously one of the present authors has pointed out that a lower-melting member among the homologous crystalline compounds may have more free space for molecular motions and consequently exhibits higher photoreactivity [36–38]. Also, the crystal density was used as a measure of the free space in crystal packing [36–39]. Besides, he studied coerced control over solid-state [2 + 2] and [4 + 4] photocyclodimerization by varying the crystal structures through formation of two-component crystals [25, 26]. As a modifier component, hydrogen-bonding intermolecular linkers (e.g., *gauche* 1,2-diamine, phthalic acid, and oxalic acid) [39–44], small molecules (e.g., NH<sub>3</sub> and divalent metal) [26, 45], and relatively small and planar molecules (e.g., imidazole, *trans,trans*-muconic acid, and acetylenedicarboxylic acid) [45, 46] were employed. In the course of these studies, two-component crystals were frequently found to be more loosely packed than one-component crystals and hence two-component crystals appeared to undergo decreased topochemical restriction to molecular motions. For example, in addition to static disorder, dynamic disorder caused by a pedal-like dynamic conformational change and volume-demanding reactions such as *trans*–*cis* photoisomerization of olefin occurred relatively easily in cocrystals [25, 26, 43, 44].

*Trans*-**1** melts at 103–104 °C and *cis*-**1** melts at 54–59 °C [15]. The lower and un-sharp melting point for *cis*-**1** may partly reflect its completely disordered crystal structure described above (Fig. 2). From the topochemical point of view on the melting point [36–38], it is expected that upon solid-state photolysis *cis*-**1** would decompose faster than *trans*-**1**. The larger librational motions ( $U_{eq}$ ) for all atoms of *cis*-**1** than those of *trans*-**1** (Table 4) might signify that *cis*-**1** would be more reactive than *trans*-**1**. However, as Eqs. 1 and

**Scheme 3** Probable decomposition pathways for *trans-1* and *cis-1***Table 3** Selected bond lengths and angles for *cis-1* and *trans-1*

Atom	Length (Å)	Atom	Angle (°)
<b>Conformer A of <i>cis-1</i></b>			
C(5)–O(1)	1.421(2)	C(5)–O(1)–O(2)	106.75(16)
C(5)–O(3)	1.436(2)	C(5)–O(3)–O(4)	108.04(16)
C(16)–O(2)	1.438(3)	O(1)–O(2)–C(16)	106.89(13)
C(16)–O(4)	1.428(2)	O(3)–O(4)–C(16)	106.84(13)
O(1)–O(2)	1.486(2)	O(1)–C(5)–O(3)	108.46(16)
O(3)–O(4)	1.470(2)	O(2)–C(16)–O(4)	107.75(17)
<b>Conformer B of <i>cis-1</i></b>			
C(5B)–O(1B)	1.434(3)	C(5B)–O(1B)–O(2B)	107.41(17)
C(5B)–O(3B)	1.444(3)	C(5B)–O(3B)–O(4B)	107.31(17)
C(16B)–O(2B)	1.431(3)	O(1B)–O(2B)–C(16B)	107.9(2)
C(16B)–O(4B)	1.423(3)	O(7)–O(8)–C(16B)	106.4(2)
O(1B)–O(2B)	1.470(2)	O(1B)–C(5B)–O(3B)	106.8(2)
O(3B)–O(4B)	1.476(2)	O(2B)–C(16B)–O(4B)	108.3(2)
<b><i>Trans-1</i></b>			
C(5)–O(1)	1.423(2)	C(5)–O(1)–O(2)	107.51(6)
C(5)–O(2 <sup>viii</sup> )	1.429(2)	O(1)–C(5)–O(2 <sup>viii</sup> )	108.50(8)
O(1)–O(2)	1.473(1)	O(1)–O(2)–C(5 <sup>viii</sup> )	107.50(6)

Symmetry code (viii) (1 – x, –y, 1 – z)

**Table 4**  $U_{eq}$  values for *cis-1* and *trans-1*

<i>Cis-1</i>		<i>Trans-1</i>	
Atom	$U_{eq}$	Atom	$U_{eq}$
<b>1,2,4,5-Tetraoxane ring</b>			
O(1)	0.0251(4)	O(2)	0.0248(4)
O(3)	0.0264(4)	O(4)	0.0250(4)
C(5)	0.0226(6)	C(16)	0.0232(6)
<b>Bu groups</b>			
C(1)	0.0556(12)	C(12)	0.0478(13)
C(2)	0.0417(10)	C(13)	0.0361(8)
C(3)	0.0316(9)	C(14)	0.0312(8)
C(4)	0.0283(7)	C(15)	0.0264(7)
<b>Ph groups</b>			
C(6)	0.0253(10)	C(17)	0.0249(9)
C(7)	0.0303(11)	C(18)	0.0283(12)
C(8)	0.0402(19)	C(19)	0.0325(13)
C(9)	0.0411(16)	C(20)	0.0272(9)
C(10)	0.038(2)	C(21)	0.0288(14)
C(11)	0.0301(13)	C(22)	0.0269(15)

3 in Scheme 2 and Fig. 4 demonstrate, *trans*-**1** decomposed initially faster than *cis*-**1** in the crystal. Recently, we have reported another topochemical factor that a locally narrow and rigid reaction cavity due to  $\pi$ - $\pi$  interactions between the neighboring aryl planes plays a crucial role in suppressing the solid-state photoreactivity of as many as seventeen 2,4,6-trialkylbenzophenones, where alkyl is *i*-Pr, Et, or Me and the corresponding benzocyclobutenols are formed [47]. Now from inspection of the crystal packing of *trans*-**1** and *cis*-**1**, it has become noticed that a similar Ph-Ph  $\pi$ - $\pi$  overlap exists for the *cis*-**1** crystal as shown in Fig. 3, but does not for the *trans*-**1** crystal. Furthermore, from the list of Table 1, *cis*-**1** ( $D_c$  1.209 g/cm<sup>3</sup>) is more densely packed than *trans*-**1** ( $D_c$  1.169 g/cm<sup>3</sup>) ( $D_c$  1.172 and 1.132 g/cm<sup>3</sup>, respectively, at 0 °C). Hence, we propose that the topochemical restriction of molecular motions by the  $\pi$ - $\pi$  interaction between the neighboring Ph planes [47] and the higher crystal packing [36–39] may be responsible for the observed lower photoreactivity of the *cis*-**1** crystal as compared with the *trans*-**1** crystal. However, it must be warned that many other factors such as defects, surface effects, different extent of light scattering, particle sizes, formation of different solid–solid mixtures/eutectic solutions are known to influence the solid-state reactivity [48–51], but the influences by these factors were not experimentally investigated in this brief report.

## Conclusion

The crystal structures of valerophenone diperoxides *trans*-**1** and *cis*-**1** were successfully solved at  $-173$  °C. The molecular structures of both the compounds adopt chair conformations. In the crystal of *cis*-**1**, the molecular structure showed whole-molecule disorder. The thermal parameters for all atoms of *cis*-**1** were slightly larger than those of *trans*-**1**.

Solid-state photolysis (with 254 nm light at 0 °C) or solution-state thermolysis (at 150 °C) of *trans*-**1** and *cis*-**1** produced valerophenone (**2**) and butyl benzoate (**3**) with the molar ratio **2/3** of 1.5–10. The observed lower **2/3** selectivity for *cis*-**1** than that for *trans*-**1** in the solid state was not explicable by the present X-ray structures. The lower solid-state photoreactivity of *cis*-**1** as compared with *trans*-**1** at the initial stage of photolysis was ascribed to the former's locally narrow and rigid reaction cavity due to the  $\pi$ - $\pi$  overlap between the neighboring Ph planes.

## Supplementary data

CCDC-787284 (*trans*-**1**) and CCDC-787283 (*cis*-**1**) contain the supplementary crystallographic data for this paper. These data can be obtained free of charge at [www.ccdc.cam.ac.uk/data\\_request/cif](http://www.ccdc.cam.ac.uk/data_request/cif) (or from the Cambridge Crystallographic

Data Centre (CCDC), 12 Union Road, Cambridge CB2 1EZ, UK; fax: +44(0) 1223-336033; e-mail: [deposit@ccdc.cam.ac.uk](mailto:deposit@ccdc.cam.ac.uk)).

**Acknowledgments** The authors are indebted to Professor Yoshiaki Matsuura (Osaka University), who first solved the crystal structure of *trans*-**1**. We also thank Dr. Sadayuki Asaoka for his assistance in doing photolysis experiments.

## References

- Ihmels H, Scheffer JR (1999) Tetrahedron 55:885–907
- Braga D, Chen S, Filson H, Maini L, Netherton MR, Patrick BO, Scheffer JR, Scott C, Xia W (2004) J Am Chem Soc 126:3511–3520
- Scheffer JR, Xia WJ (2005) Top Curr Chem 254:233–262
- Tanaka K, Toda F (2000) Chem Rev 100:1025–1074
- Toda F, Tanaka K, Miyamoto H (2001) In: Schanze KS (ed) Understanding and manipulating excited-state processes, vol 8. Marcel Dekker, New York, 2001, p. 385
- MacGillivray LR (2008) J Org Chem 73:3311–3317
- MacGillivray LR, Papaefstathiou GS, Friscic T, Hamilton TD, Bucar DK, Chu Q, Varshney DB, Georgiev IG (2008) Acc Chem Res 41:280–291
- Georgiev IG, MacGillivray LR (2007) Chem Soc Rev 36:1239–1248
- Lauher JW, Fowler FW, Goroff NS (2008) Acc Chem Res 41:1215–1229
- Kim HS, Shibata Y, Wataya Y, Tsuchiya K, Masuyama A, Nojima MJ (1999) J Med Chem 42:2604–2609
- Vennerstrom JL, Fu HN, Ellis WY, Ager AL Jr, Wood JK, Andersen SL, Gerena L, Milhous WK (1992) J Med Chem 35:3023–3027
- O'Neill PM, Amewu RK, Nixon GL, ElGarah FB, Mungthin M, Chadwick J, Shone AE, Vivas L, Lander H, Barton V, Muangnoicharoen S, Bray PG, Davies J, Park BK, Wittlin S, Brun R, Preschel M, Zhang K, Ward SA (2010) Angew Chem Int Ed 49:5693–5697
- Kim HS, Tsuchiya K, Shibata Y, Wataya Y, Ushigoe Y, Masuyama A, Nojima M, McCullough KJ (1999) J Chem Soc Perkin Trans 1(13):1867–1870
- Badawi HM, Al-Saadi AA, Ali AS (2010) J Mol Struct 969:197–203
- Ito Y, Konishi M, Matsuura T (1979) Photochem Photobiol 30:53–57
- Ito Y, Matsuura T, Yokoya H (1979) J Am Chem Soc 101:4010–4011
- Ito Y, Yokoya H, Umehara Y, Matsuura T (1980) Bull Chem Soc Jpn 53:2407–2408
- Ito Y, Tone M, Yokoya H, Matsuura T, Schuster GB (1986) J Org Chem 51:2240–2245
- Altomare A, Burla M, Camalli M, Casciarano G, Giacovazzo C, Guagliardi A, Moliterni A, Polidori G, Spagna R (1999) J Appl Crystallogr 32:115–119
- Sheldrick GM (2008) Acta Crystallogr A 64:112–122
- CrystalStructure 3.8, Crystal Structure Analysis Package; Rigaku and Rigaku Americas (2000–2007): 9009 New Trails Dr., The Woodlands, TX 77381, USA
- Kabuto C, Akine S, Nemoto T, Kwon E (2009) J Cryst Soc Jpn 51:218–224
- Macrae CF, Edgington PR, McCabe P, Pidcock E, Shields GP, Taylor R, Towler M, van de Streek J (2006) J Appl Crystallogr 39:453–457

24. Spek AL (2009) *Acta Crystallogr D* 65:148–155
25. Ito Y (1998) *Synthesis* 1:1–32
26. Ito Y (1999) In: Ramamurthy V, Schanze KS (eds) *Molecular and supramolecular photochemistry*, vol 3. Marcel Dekker, New York, pp 1–70
27. Cremer D, Pople JA (1975) *J Am Chem Soc* 97:1354–1358
28. Mackay AL (1984) *Acta Crystallogr A* 40:165–166
29. Fischer RX, Tillmanns E (1988) *Acta Crystallogr C* 44:775–776
30. Wagner PJ (1971) *Acc Chem Res* 4:168–177
31. McCullough KJ, Morgan AR, Nonhebel DC, Pauson PL (1980) *J Chem Res (S)* 35–37
32. Miura M, Nojima M, Kusabayashi S (1980) *JCS Perkin 1*:1950–1954
33. Cafferata LFR, Eyley GN, Mirifico MV (1984) *J Org Chem* 49:2107–2111
34. Cafferata LFR, Eyley GN, Svartman EL, Canizo AI, Borkowski EJ (1990) *J Org Chem* 55:1058–1061
35. Ishiguro K, Nojima T, Sawaki Y (1997) *J Phys Org Chem* 10:787–796
36. Ito Y, Ito H, Ino M, Matsuura T (1988) *Tetrahedron Lett* 29:3091–3094
37. Matsuura T, Meng J, Ito Y, Irie M, Fukuyama K (1987) *Tetrahedron* 43:2451–2456
38. Ito Y (1989) In: Anpo M, Matsuura T (eds) *Photochemistry on solid surfaces*. Elsevier, Amsterdam, pp 469–480
39. Ito Y, Borecka B, Scheffer JR, Trotter J (1995) *Tetrahedron Lett* 36:6083–6086
40. Ito Y, Borecka B, Olovsson G, Trotter J, Scheffer JR (1995) *Tetrahedron Lett* 36:6087–6090
41. Ito Y (1996) *Mol Cryst Liq Cryst* 277:247–253
42. Ito Y, Olovsson G (1997) *J Chem Soc Perkin Trans 1*(11):127–133
43. Ito Y, Hosomi H, Ohba S (2000) *Tetrahedron* 56:6833–6844
44. Ohba S, Hosomi H, Ito Y (2001) *J Am Chem Soc* 123:6349–6352
45. Ito Y, Kitada T, Horiguchi M (2003) *Tetrahedron* 59:7323–7329
46. Horiguchi M, Ito Y (2006) *J Org Chem* 71:3608–3611
47. Ito Y, Takahashi H, Hasegawa J, Turro NJ (2009) *Tetrahedron* 65:677–689
48. Garcia-Garibay MA (2003) *Acc Chem Res* 36:491–498
49. Garcia-Garibay MA (2007) *Angew Chem Int Ed* 46:8945–8947
50. Kuzmanich G, Natarajan A, Chin K, Veerman M, Mortko CJ, Garcia-Garibay MA (2008) *J Am Chem Soc* 130:1140–1141
51. Lebedeva NV, Tarasov VF, Resendiz MJE, Garcia-Garibay MA, White RC, Forbes MDE (2010) *J Am Chem Soc* 132:82–84